Complexes of Heteroscorpionate Trispyrazolylborate Ligands. Part 10. Structures and Fluxional Behavior of Rhodium(I) Complexes with Heteroscorpionate Trispyrazolylborate Ligands, Tp″Rh(LL) (LL = $(CO)_2$ or COD)

Tomasz Ruman,[†] Zbigniew Ciunik,[‡] Anna M. Trzeciak,[‡] Stanisław Wołowiec,*[,†,‡] and Józef J. Ziółkowski*[,‡]

Faculty of Chemistry, Rzeszów University of Technology, 6 Powstańców Warszawy Avenue, 35-959 Rzeszów, Poland, and Faculty of Chemistry, University of Wrocław, 14 Joliot-Curie Street, 50-383, Wrocław, Poland

Received October 22, 2002

Heteroscorpionate Tp″ ligands constructed of two 3-phenyl-5-methylpyrazolyl and a variable third pyrazolyl residue (3-methyl-5-phenyl-, 3,5-dimethyl-, and 3,5-diethylpyrazolyl) coordinate to rhodium(I) in a κ^2 fashion to form Tp″Rh(LL) complexes (where LL = COD or $(CO)_2$). One of the two 3-phenyl-5-methylpyrazolyl and the less sterically hindered pyrazolyl coordinate through N(2) atoms, while the axially appended 3-phenyl-5-methylpyrazolyl is in side-on conformation. The Tp″Rh(COD) complexes possess C_1 symmetry in the solid state. The energy of activation of the exchange between coordinated and uncoordinated pyrazolyls was estimated from variable-temperature ^{1}H NMR measurements. Two $\Delta G^{\ddagger}$ values were found for heteroscorpionate complexes. The $\Delta G^{\ddagger}_1 - \Delta G^{\ddagger}_2$ depends on a difference in steric demands of competing pyrazoles. For the homoscorpionate $Tp^{Ph,Me}$Rh(COD) complex two rotational isomers were identified by low-temperature ^{1}H NMR spectroscopy, which originate from slow rotation of the dangling 3-phenyl-5-methylpyrazolyl residue. All studied Tp′Rh(COD) complexes were found to be catalytically active in regioselective polymerization of phenylacetylene.

Introduction

The chemistry of transition metal ion complexes with the trispyrazolylborate anion (Tp) was initiated by Trofimenko in 1966.[1] Structural modifications of pyrazolyl residues (pz) by introducing various substituents at the 3−5 positions of pz resulted in obtaining the homoscorpionate ligands named second-generation trispyrazolylborates (Tp′), which possess C_{3v} symmetry, and heteroscorpionates, ligands of C_s symmetry, constructed of two different pyrazolyl residues.[2] The latter will be called third-generation trispyrazolylborates (Tp″) hereafter. Heteroscorpionates are obtainable from asymmetric 3-R^1,5-R^2pzH upon condensation with borohydride (spontaneously formed Tp″) or on the same route with the use of two different pyrazoles ("synthetic" heteroscorpionates). Transition metal ion compounds with spontaneous Tp″ can be prepared by ligation of pure Tp″ (usually sodium or thallium(I) salts of Tp″ are used) or by thermally induced intramolecular conversion of homoscorpionate into heteroscorpionate in the complex.[3,4] The property of 3-R^1-5-R^2-pyrazol-1-yl residues to undergo such borotropic shifts into 3-R^2-5-R^1-pyrazol-1-yl has been recently explored in detail and eventually used to obtain the chiral Tp* ligand with boron-centered chirality: hydro(3,5-dimethylpyrazolyl)(3-isopropyl-5-phenylpyrazolyl)(3-phenyl-5-isopropylpyrazolyl)borate from synthetic Tp″, hydrobis(3-phenyl-5-isopropylpyrazolyl)(3,5-dimethylpyrazolyl)borate.[5] The goal has been achieved by thermal conversion of the corresponding Tp″Co(NCS) complex under mild conditions. The Tp″'s are also interesting ligands for transition metal ions which engage two nitrogen donors of these anions. In such a case one may expect the preferential coordination of two pyrazolyl residues with smaller steric hindrance imposed by 3- and/or 5-substituents of Tp″. In this paper we have described the structures and fluxional behavior of a series of Tp″Rh(LL) complexes, where LL = $(CO)_2$ or COD. The Tp″ ligands were constructed of two 3-phenyl-5-methylpyrazolyl residues and a variable third one: 3,5-dimethyl-, 3,5-diethyl-, and 3-methyl-5-phenylpyrazolyl. For comparison the previously known $Tp^{Ph,Me}$Rh(COD) complex was also studied.

Results and Discussion

Substituted tris(pyrazol-1-yl)borates (second-generation scorpionates, Tp′)[2] form Tp′Rh(LL) complexes, in

[†] Rzeszów University of Technology.
[‡] University of Wrocław.

(1) Trofimenko, S. *J. Am. Chem. Soc.* **1966**, *88*, 1842.
(2) Trofimenko, S. *Scorpionates: the coordination chemistry of polypyrazolylborate ligands*; Imperial College Press: London, U.K., 1999.
(3) Trofimenko, S.; Calabrese, J. C.; Domaille, P. J.; Thompson, G. S. *Inorg. Chem.* **1989**, *28*, 1091.
(4) Ruman, T.; Łukasiewicz, M.; Ciunik, Z.; Wołowiec, S. *Polyhedron* **2001**, *20*, 2551.
(5) Ruman, T.; Ciunik, Z.; Wołowiec, S. *Eur. J. Inorg. Chem.*, submitted.

10.1021/om020873x CCC: $25.00
Publication on Web 01/31/2003

Scheme 1

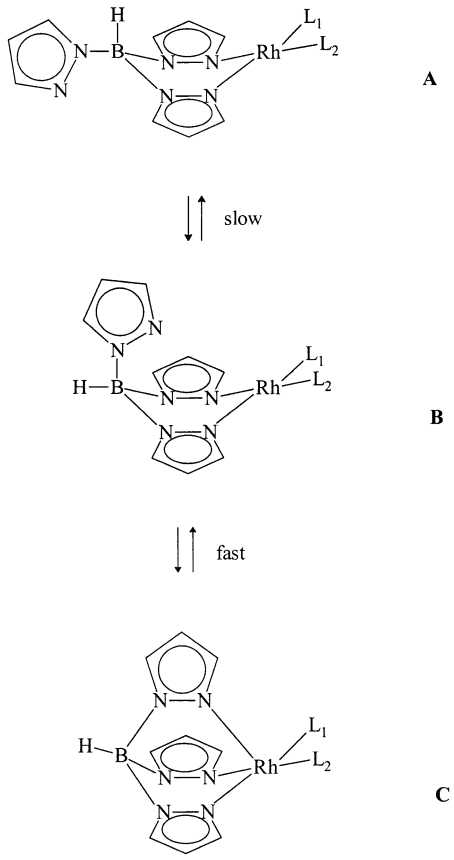

which they coordinate in κ^2 fashion, when $L_1L_2 = (CO)_2$ or COD. The ^{1}H NMR and IR studies of those complexes in solution demonstrate that homoscorpionate Tp′ interconverts between forms A, B, and C (Scheme 1). The conversion B ↔ C is fast on the ^{1}H NMR time scale, resulting in averaging of all pyrazolyl resonances, whereas the A ↔ B interconversion is relatively slower and the ^{1}H NMR spectra indicate the presence of two sets of resonances of 2:1 intensity ratio for A. In the solid state the isomers A were evidenced by X-ray crystallography barely in two cases, i.e., for $Tp^{Ph}Rh(COD)$ and $Tp^{Menth}Rh(CO)_2$.[6,7] However in solution both of these compounds indicate the presence of both A and averaged B ↔ C species at concentrations depending on temperature and solvent. Here we have applied the heteroscorpionate Tp″ ligands to construct Tp″Rh(LL) complexes and studied their properties in structural and fluxional aspects.

Structures of 1−4. The complex [HB(3-Ph,5-Mepz)$_2$-(3,5-diMepz)]Rh(CO)$_2$ (**1**) was obtained by the procedure used previously for the synthesis of $Tp^{Ph,Me}Rh(CO)_2$,[8] i.e., with Rh(acac)(CO)$_2$ as starting material, whereas [RhCl(COD)]$_2$ was used for the synthesis of $Tp^{Ph,Me}$Rh-(COD) (**2**), [HB(3-Ph,5-Mepz)$_2$(3-Me,5-Phpz)]Rh(COD) (**3**), and [HB(3-Ph,5-Mepz)$_2$(3,5-diEtpz)] Rh(COD) (**4**), where ([HB(3-Ph,5-Mepz)$_2$(3,5-diMepz)] = hydrobis(3-phenyl-5-methylpyrazol-1-yl)(3,5-dimethylpyrazol-1-yl)-borate, [HB(3-Ph,5-Mepz)$_2$(3-Me,5-Phpz)] = hydrobis(3-phenyl-5-methylpyrazol-1-yl)(3-methyl-5-phenylpyrazol-1-yl)borate, and [HB(3-Ph,5-Mepz)$_2$(3,5-diEtpz)] = hydrobis(3-phenyl-5-methylpyrazol-1-yl)(3,5-diethylpyrazol-1-yl)borate. Monocrystals suitable for crystallographic studies were obtained for all complexes. A view of **1** is presented at Figure 1. The 3,5-diMepz and one of two 3-Ph,5-Mepz moieties of Tp″ are coordinated by N(4) and N(2) donors, respectively. The Rh−N(4) bond is shorter by 0.01 Å in comparison with the Rh−N(2) one. The nitrogen atom of appended 3-Ph,5-Mepz weakly interacts with Rh(I) (2.84 Å). Its 3-phenyl substituent is almost coplanar with the pyrazolyl ring and bisects the OC−Rh−CO angle.

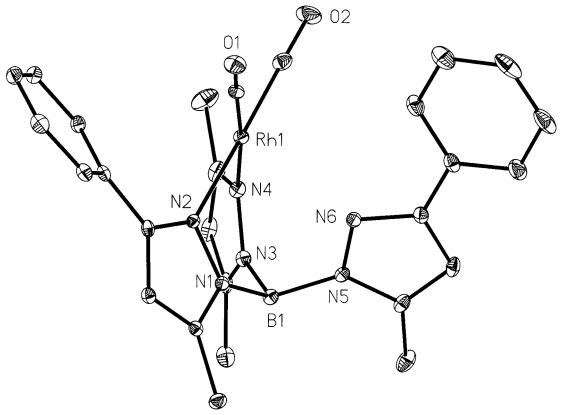

Figure 1. View of **1**. Selected bond lengths (Å) and angles (deg): Rh(1)−C(27), 1.852(2); Rh(1)−C(26), 1.862(2); Rh-(1)−N(4), 2.0855(16); Rh(1)−N(2), 2.0957(16); C(27)−Rh-(1)−C(26), 88.35(9); C(27)−Rh(1)−N(4), 94.79(8); C(26)−Rh(1)−N(4), 174.79(7); C(27)−Rh(1)−N(2), 178.79(7); C(26)−Rh(1)−N(2), 90.69(7); N(4)−Rh(1)−N(2), 86.11(6).

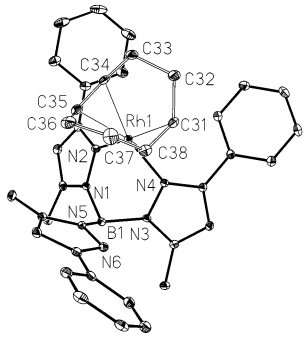

Figure 2. View of **2**. Selected bond lengths (Å) and angles (deg): Rh(1)−N(2), 2.0950(15); Rh(1)−N(4), 2.1003(14); Rh-(1)−C(38), 2.1344(19); Rh(1)−C(31), 2.1355(18); Rh(1)−C(35), 2.1395(19); Rh(1)−C(34), 2.1457(17); N(2)−Rh(1)−N(4), 82.60(6); N(2)−Rh(1)−C(38), 154.03(7); N(4)−Rh(1)−C(38), 96.33(7); N(2)−Rh(1)−C(31), 167.48(7); N(4)−Rh(1)−C(31), 92.93(6); N(2)−Rh(1)−C(35), 91.48(7); N(4)−Rh(1)−C(35), 161.04(7); N(2)−Rh(1)−C(34), 98.68(6); N(4)−Rh(1)−C(34), 160.85(7).

The molecular structure of **2** is presented in Figure 2. The Rh−N(3-Ph,5-Mepz) bond lengths in **2** are typical for Tp′Rh(COD) complexes (about 2.10 Å, column 3 in Table 1) and differ slightly from each other; Rh−N(4) and Rh−N(2) distances are 2.100 and 2.095 Å, respectively. The only reasonable explanation for this difference is the involvement of asymmetric arrangement of the uncoordinated pyrazolyl moiety, the motif observed in all homoscorpionate Tp′Rh(COD) complexes.

(6) Sanz, D.; Santa Maria, M. D.; Claramunt, R. M.; Cano, M.; Heras, J. V.; Campo, J. A.; Ruiz, F. A.; Pinilla, E.; Monge A. *J. Organomet. Chem.* **1996**, *526*, 341.

(7) Keyes, M. C.; Young, V. G.; Tolman, W. B. *Organometallics* **1995**, *15*, 4133.

(8) Moszner, M.; Wolowiec, S.; Trösch., A.; Vahrenkamp, H. *J. Organomet. Chem.* **2000**, *595*, 178.

Table 1. X-ray Crystallographic Data and Metric Parameters for Tp′Rh(L_1L_2) Complexes

	complex[ref]	Rh−N(pz) [Å]	Rh−X [Å][a]	α [deg][b]	*D* (g) [Å][c]	ϵ [deg][d]	δ [deg][e]	χ[deg][f]
1	$[B(pz)_4]$Rh(COD)[9,g]	2.099, 2.099, 3.694[h]	2.012, 2.012	105.7	0.038 (0.000)	1.5, 1.5	3.0	74.4
2	Bp^{cod}Rh(COD)[10]	2.107, 2.107	2.004, 2.004		0.098 (0.000)	9.9, 9.9	0.8	
3	$Tp^{Ph,Me}$Rh(COD), **2**[j]	2.086, 2.096, 3,767[h]	2.019, 2.027	109.5	0.060 (0.067)	6.9, 19.7	7.2	77.4
4	[HB(3-Ph,5-Mepz)$_2$(3-Me,5-Phpz)]Rh-(COD), **3**[j]	2.098, 2.100, 3.709[h]	2.014, 2.034	107.9	0.064 (0.053)	23.5, 0.5	6.5	76.6
5	HB(3-Ph,5-Mepz)$_2$(3,5-diEtpz)]Rh-(COD), **4**[j]	2.083, 2.095, 3.868[h]	2.019, 2.030	110.9	0.090 (0.117)	19.2, 15.2	11.9	79.7
6	Tp^{iPr2}Rh(COD)[11]	2.098, 2.133, 3.718[h]	2.025, 2.016	110.0	0.326 (0.149)	4.9, 10.5	12.5	74.4
7	$Tp^{Me,mt4}$Rh(COD)[12,k]	2.082, 2.133, 3.778[h]	2.011, 2.005	112.3	0.028 (0.157)	5.4, 14.5	13.1	75.3
8	$Tp^{4Bo,3Me}$Rh(COD)[113,m]	2.106, 2.120, 3.782[h]	2.026, 2.010	125.0	0.022 (0.169)	9.5, 15.0	14.1	76.2
9	Tp^{Ph}Rh(COD)[6]	2.094, 2.094, 5.395[n]	2.024, 2.017	151.1	0.164 (0.017)	8.9, 15.1	12.6	171.3
10	[HB(3-Ph,5-Mepz)$_2$(3,5-diMepz)]Rh-(CO)$_2$, **1**[j]	2.086, 2.096, 2.840[h]	1.852, 1.862	90.0	0.043 (0.029)	15.8, 21.4	4.2	81.0
11	Tp^{p-An}Rh(CO)$_2$[14]	2.110, 2.107, 2.578[h]	1.824, 1.841	93.1	0.121 (0.054)	1.3, 1.4	10.7	77.9
12	Tp^{a}Rh(CO)$_2$[15,p]	2.093, 2.091, 2.780[h]	1.855, 1.844	89.1	0.045 (0.020)	6.1, 6.2	4.0	81.2
		2.109,2.105, 2.641[h]	1.851, 1.847	90.2	0.096 (0.015)	2.5, 10.1	7.8	82.2
13	$Tp^{CF3,Me}$Rh(CO)$_2$[16]	2.114, 2.115, 2.637[h]	1.824, 1.831	88.5	0.064 (0.043)	5.6, 16.6	6.3	81.3
14	$Tp^{Ph,Me}$Rh(CO)$_2$[8]	2.098, 2.102, 2.835[h]	1.851, 1.851	90.8	0.071 (0.061)	17.1, 17.7	7.7	80.8
15	Tp^{Menth}Rh(CO)$_2$[7,r]	2.083, 2.104, 5.459[n]	1.853, 1.855	163.5	0.065 (0.027)	2.6, 12.2	5.7	174.5

[a] Rh−C or Rh−(center of C═C) distance. [b] Boron-centered bite angle calculated as $2/3\sum_{i=1}^{3}\alpha_i$, where α_i is the angle between the Rh−B and B−N(2) of pz lines. [c] Out-of-plane displacement of rhodium; the mean plane is defined by four donor atoms (or center of double bond of COD ligand); the values in parentheses show the goodness of the plane. [d] Pyrazole twist described by Rh−N(2)−N(1)−B dihedral angles. [e] Metric parameter describing deformation of the coordination plane, the dihedral angle between $(N)_2$−Rh and Rh−$(C)_2$ (or Rh−(center of C═C) planes. [f] Angle between Rh···B axis and B−N(1) of the appended pyrazolyl moiety. [g] Bp^{cod} = (cyclooctane-1,5-diyl)bis(pyrazol-1-yl)borate. [h] Uncoordinated axial pyrazolyl moiety. [j] This work. [k] $Tp^{Me,mt4}$ = tris(3-methyl-4,5-(1,3-butylene)pyrazol-1-yl)borate. [m] $Tp^{4Bo,3Me}$ = hydrotris(3-methylindazol-1-yl)borate. [n] Uncoordinated equatorial pyrazolyl moiety. [p] Tp^{a} = hydrotris(2*H*-benz[*g*]-4,5-dihydroindazol-2-yl)borate, two independent molecules. [r] Tp^{Menth} = hydrotris(mentho(2,3-*c*)pyrazol-1-yl)borate.

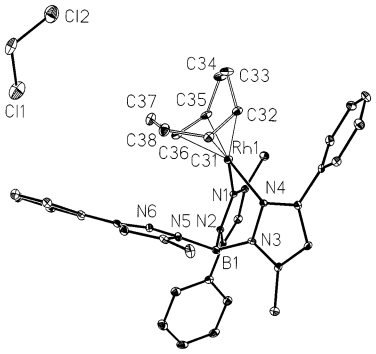

Figure 3. View of **3**·CH_2Cl_2. Selected bond lengths (Å) and angles (deg): Rh(1)−N(1), 2.098(2); Rh(1)−N(4), 2.100(2); Rh(1)−C(36), 2.129(3); Rh(1)−C(35), 2.130(3); Rh(1)−C(31), 2.136(3); Rh(1)−C(32), 2.162(3); N(1)−Rh(1)-N(4), 82.58-(8); N(1)−Rh(1)−C(36), 95.37(10); N(4)−Rh(1)−C(36), 154.57-(10); N(1)−Rh(1)−C(35), 92.03(10); N(4)−Rh(1)−C(35), 166.57(10); N(1)−Rh(1)−C(31), 160.29(9); N(4)−Rh(1)−C(31), 92.30(10); N(1)−Rh(1)−C(32), 162.09(10); N(4)−Rh-(1)−C(32), 99.77(10).

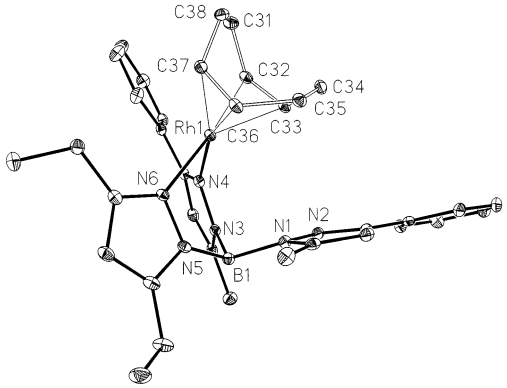

Figure 4. View of **4**. Selected bond lengths (Å) and angles (deg): Rh(1)−N(6), 2.0831(14); Rh(1)−N(4), 2.0953(15); Rh-(1)−C(33), 2.1284(17); Rh(1)−C(36), 2.1377(17); Rh(1)−C(32), 2.1425(17); Rh(1)−C(37), 2.1516(18); N(6)−Rh(1)−N(4), 81.55(6); N(6)−Rh(1)−C(33), 149.43(7); N(4)−Rh(1)−C(33), 97.22(6); N(6)−Rh(1)−C(36), 89.90(6); N(4)−Rh(1)−C(36), 161.81(7); N(6)−Rh(1)−C(32), 170.91(7); N(4)−Rh(1)−C(32), 92.73(6); N(6)−Rh(1)−C(37), 102.06(6); N(4)−Rh(1)−C(37), 160.15(7).

The molecular structures of **3**·CH_2Cl_2 and **4** are presented in Figures 3 and 4, respectively. Both complexes are built of Tp″ ligands with two 3-Ph,5-Mepz residues and a third one of lower steric hindrance (3-Me,5-Phpz in **3**·CH_2Cl_2 and 3,5-diEtpz in the case of **4**). The Tp″ ligands are coordinated in κ^2 manner with side-on appended 3-Ph,5-Mepz residues. The Rh−N(pyrazolyl) bond lengths differ slightly within the molecules of **3**·CH_2Cl_2 and **4**. There are three factors influencing these bond lengths: a different steric hindrance imposed by 3-R (and 5-R) substituents of coordinated pyrazolyl residues, different electronic *cis*−*trans* effects resulting from nonequivalent in-plane pyrazolyls, and conformation of uncoordinated 3-Ph,5-Mepz, as it was already found in the molecule of **2**. Those bond lengths are equal within the complexes $[B(pz)_4]$Rh(COD) and Bp^{cod}Rh-(COD) (where Bp^{cod} = cyclooctane-1,5-diylbis(pyrazolyl)-borate, entries 1 and 2 in Table 1), in which the mentioned differential factors do not operate.

Generally, for all Tp′Rh(COD) complexes with axially appended pyrazolyl residues the uncoordinated pyrazolyls are arranged in a near side-on conformation, which allows the N(2) of the pyrazole to interact weakly with the rhodium(I) ion at a distance of 3.709−3.868 Å (entries 3−8, column 3 in Table 1). Also the Rh(I)−(C═C) distances (measured in relation to the center of the C═C bond, column 4) are slightly variable within the 2.005−2.027 Å range.

Similar relationships can be found for Tp′Rh$(CO)_2$ complexes (entries 10−14), for which, however, the Rh-(I)−N(2) axial uncoordinated pyrazole distance is considerably shorter and varies within 2.578−2.840 Å, whereas the Rh(I)−C bond lengths vary within the

1.824−1.862 Å range. Thus, the ligands interact with the rhodium(I) metal center more strongly in the case of Tp′Rh(CO)$_2$ than that in Tp′Rh(COD). This can also be concluded on the basis of comparison of "bite" angle α (column 5), which is considerably smaller for dicarbonyl complexes (for precise comparison see entries 3 and 14). These comparisons clearly indicate the involvement of higher steric demands from COD ancillary ligands in comparison with those of (CO)$_2$.

The coordination sphere in both types of complexes is slightly distorted from planarity; the rhodium metal ion is 0.022−0.121 Å displaced out of the mean plane with the exception of the high value for Tp^{iPr2}Rh(COD) (0.326 Å, entry 6).

Close insight into the boat conformation of the B−(N(1)−N(2))$_2$−Rh fragment measured by the two dihedral angles B−N(1)−N(2)−Rh (ϵ, column 6), which can be described as a pyrazole twist, indicates that pyrazolyl substituents induce considerable distortions of the boat. Consequently, the distortion of the coordination sphere around the central metal ion occurs, as measured by the dihedral angle between two planes: Rh−N(pz)$_2$ and Rh−(C═C)$_2$ in the case of Tp′Rh(COD) or Rh−C in the case of Tp′Rh(CO)$_2$ (angle δ in column 8). The values of δ are again larger for Tp′Rh(COD) compounds than those for Tp′Rh(CO)$_2$.

All the metric parameters are considerably different in the case of Tp′Rh(L$_1$L$_2$) complexes with equatorial uncoordinated pyrazole (entries 9 and 15). The angle χ between the rhodium−boron axis and the boron−N(1) bond of appended pyrazole distinguishes the conformation of the Tp′ ligand; for conformers B the value of χ varies within 74.4−82.2°, whereas it is larger than 170° in the case of Tp′ in conformation A.

^{1}H NMR Studies. Tp′Rh(L$_1$L$_2$) complexes (where L$_1$L$_2$ = diene or (CO)$_2$) have been extensively studied by NMR technique.[8,11,13−21] The ^{1}H NMR spectra of homoscorpionate complexes showed only one set of resonances from pyrazolyl residues, evidencing the presence of either exclusively B ↔ C species in solution or fast interconverting A ↔ B ↔ C. These kind of spectra were observed at ambient temperature for TpRh(COD),[17] Tp^{Me,Me}Rh(COD),[18] Tp^{Me,Me,4Cl}Rh(COD),[17] Tp^{CF3,Me}Rh(COD),[17] Tp^{CF3,CF3}Rh(COD),[16] Tp^{i}PrRh(COD),[11] Tp^{iPr,iPr}Rh(COD),[21] Tp^{4Bo,3Me}Rh(COD),[13] Tp^{Ph,Ph}Rh(COD),[20] Tp^{Ph,Me}Rh(COD),[15,17] and their Ir(I) analogues.[19] Exceptionally, the presence of pure B form at ambient temperature was evidenced in the case of Tp^{Ms}Rh(COD), resulting in the appearance of two sets of resonances from pyrazolyl moieties of 2:1 intensity ratio,[21] whereas two separate spectra of isomer A and averaged B ↔ C were observed for Tp^{Ph}Rh(COD)[6] and Tp^{pAn}Rh(COD)[14] at a percentage depending on temperature and solvent. In some cases the fluxional behavior of Tp′Rh(L$_1$L$_2$) complexes was studied, indicating that in the case of Tp′Rh(CO)$_2$ the A ↔ B ↔ C was fast at available low temperatures.[8] Interestingly, in the highly sterically hindered molecule of Tp^{Menth}Rh(CO)$_2$ two separate spectra of B ↔ C (one set of pz resonances) and A (three sets of pz resonances due to C_1 symmetry of the species) were observed below the coalescence temperature in toluene.[7] In the case of heteroscorpionate Tp″M(COD) complexes (M = Rh, Ir) two sets of pyrazolyl resonances of 2:1 intensity ratio were observed for [HB(3-^{i}Pr,4-Brpz)$_2$(5-^{i}Pr,4-Brpz)]Rh(COD),[17] [HB(3-Mepz)$_2$(5-iMez)]Ir(COD),[19] and [HB(3-Mepz)(5-iMez)$_2$]Ir(COD),[19] although in the case of [HB(3-Mespz)$_2$(5-Mespz)]Rh(COD)[21] three unexplained 4-H(pz) resonances of 2:2:1 intensity ratio were found. Three resonances from the ancillary COD ligand were present, consistently with fast interconverting B ↔ C or A ↔ B ↔ C systems including the Tp″Rh(COD) complexes, while doubling of resonances for inert A species was observed according to their C_s symmetry.

The ^{1}H NMR spectrum of **1** comprises two 4-H resonances at 6.33 and 6.02 ppm of 2:1 intensity ratio attributed to 4-H(3-Ph,5-Mepz) and 4-H(3,5-diMepz), respectively. The variable-temperature experiments performed in toluene-d_8 revealed that **1** remained in fast exchange between B ↔ C even at 190 K on the time scale of the method. Similar behavior was found previously in the case of Tp^{Ph,Me}Rh(CO)$_2$, whereas the slow, solvent-dependent isomerization of average B ↔ C species into the A form has been found in the case of Tp^{Ph}Rh(CO)$_2$, resulting in evolution of the ^{1}H NMR spectrum of pure B ↔ C species with a characteristic broad 4-H singlet into two doublets of 2:1 intensity ratio attributed to the A isomer.[6] The isomer A was not found for **1** in any common solvent used. On the basis of this observation one may conclude that the presence of the 5-methyl substituent on pyrazolyl moieties destabilizes conformation A.

The ^{1}H NMR spectrum of Tp^{Ph,Me}Rh(COD) (**2**, Figure 5) reveals the presence of averaged species B ↔ C down to 228 K in dichloromethane-d_2, as demonstrated by the presence of a 4-H singlet at 6.29 ppm. Also one set of resonances from COD is observed at temperatures above 228 K. Below that point two resonances of 4-H(3-Ph,5-Mepz) appear and simultaneously the number of resonances from the COD ligand doubles. This situation corresponds to a slow chemical exchange between coordinated and dangling pyrazolyl residues. Surprisingly, the molecule loses its C_s symmetry below the 207 coalescence point, resulting in the appearance of three 4-H(3-Ph,5-Mepz) resonances and 12 COD resonances. The only reason responsible for further dissymmetry is slow rotation of the dangling pyrazolyl residues around the B−N(pz) bond. Estimated values for energy of

(9) Cocivera, M.; Ferguson, G.; Kaitner, B.; Lalor, F. J.; O'Sullivan, D. J.; Parvez, M.; Ruhl, B. *Organometallics* **1982**, *1*, 1132.
(10) Bortolin, M.; Bucher, U. E.; Rüegger, H.; Venanzi, L. M.; Albinati, A.; Lianza, F.; Trofimenko, S. *Organometallics* **1992**, *11*, 2514.
(11) Akita, M.; Ohta, K.; Takahashi, Y.; Hikichi, S.; Moro-oka, Y. *Organometallics* **1997**, *16*, 4121.
(12) Rheingold, A. L.; Liable-Sands, L.; Trofimenko, S. *Inorg. Chem.* **2000**, *39*, 1333.
(13) Rheingold, A. L.; Haggerty, B. S.; Yap, G. P. A.; Trofimenko, S. *Inorg. Chem.* **1997**, *36*, 5097.
(14) Santa Maria, M. D.; Claramunt, R. M.; Campo, J. A.; Criado, R.; Heras, J. V.; Ovejero, P.; Pinilla, E.; Torres, M. R. *J. Organomet. Chem.* **2000**, *605*, 117.
(15) Rheingold, A. L.; Ostrander, R. L.; Haggerty, B.; Trofimenko, S. *J. Am. Chem. Soc.* **1994**, *33*, 3666.
(16) Del Ministro, E.; Renn, O.; Rüegger, H.; Venanzi, L. M.; Burckhardt, U.; Gramlich, V. *Inorg. Chim. Acta* **1995**, *240*, 631.
(17) Bucher, U. E.; Currao, A.; Nesper, R.; Rüegger, H.; Venanzi, L. M.; Younger, E. *Inorg. Chem.* **1995**, *34*, 66.
(18) Boaretto, R.; Ferrari, A.; Merlin, M.; Sostero, S.; Traverso, O. *J. Photochem. Photobiol. A* **2000**, *135*, 179.
(19) Albinati, A.; Bovens, M.; Rüegger, H.; Venanzi, L. M. *Inorg. Chem.* **1997**, *36*, 5991.
(20) Katayama, H.; Yamamura, K.; Miyaki, Y.; Ozawa, F. *Organometallics* **1997**, *16*, 4497.
(21) Rheingold, A. L.; White, C. B.; Trofimenko, S. *Inorg. Chem.* **1993**, *32*, 3471.

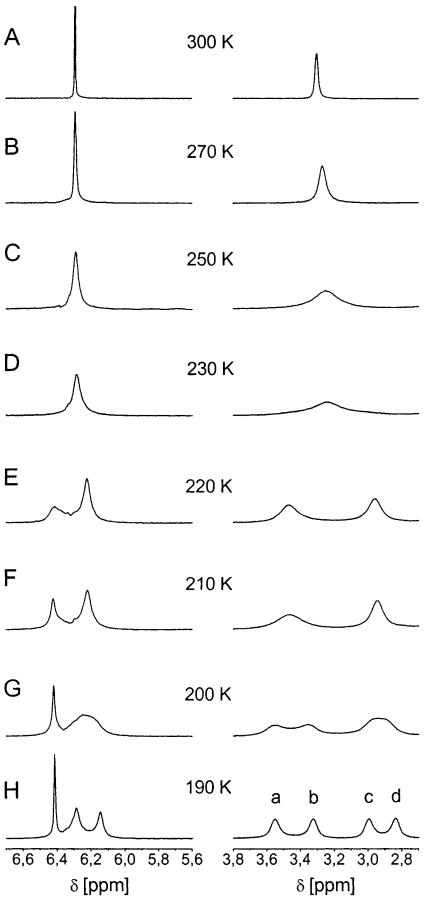

Figure 5. Selected regions of the ^{1}H NMR spectra of **2** (dichloromethane-d_2): the 4-H(pz) resonances (left column) and 1′,2′,5′,6′-H(COD) resonances (right column).

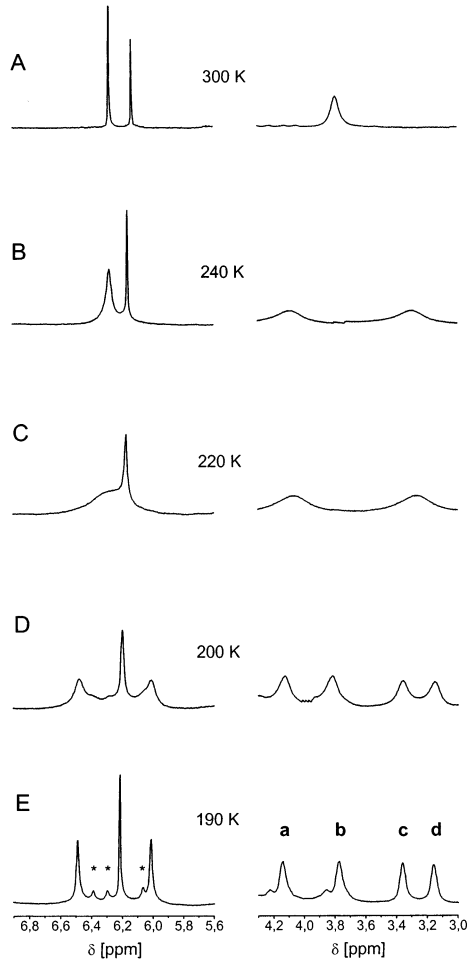

Figure 6. Selected regions of the ^{1}H NMR spectra of **3** (dichloromethane-d_2): the 4-H(pz) resonances (left column) and 1′,2′,5′,6′-H(COD) resonances (right column). The 4-H(pz) resonances from the minor DR isomer are labeled with asterisks.

activation for pyrazolyl exchange and rotation of dangling pyrazole were $\Delta G^{\ddagger}_{BC} = 43.2$ kJ/mol and $\Delta G^{\ddagger}_{DR} = 43.9$ kJ/mol, respectively (DR, dangling rotational isomer). The COSY spectrum taken at 190 K for **2** indicated that scalar coupling occurs within olefinic protons a ↔ d and b ↔ c (see assignments in bottom trace of Figure 5), while EXSY cross-peaks were found within all four sets of a ↔ b ↔ c ↔ d of protons in the NOESY spectrum at the same temperature. Thus, the chemical shift nonequivalence caused by up-and-down asymmetry in **2** is much larger (for individual pairs of vicinal olefinic COD protons at 190 K: $\Delta\delta_{ad} = \delta_a - \delta_d = 0.72$ ppm and $\Delta\delta_{bc} = \delta_b - \delta_c = 0.32$ ppm, and average $\Delta\delta_{BC} = (\delta_a + \delta_b)/2 - (\delta_c + \delta_d)/2 = 0.52$ and 0.51 ppm at 220 K) in comparison with that resulting from slowly rotating asymmetric uncoordinated 3-Ph,5-Mepz (0.04 ppm, measured as $\Delta\delta_{DR} = (\delta_a + \delta_d)/2 - (\delta_b + \delta_c)/2$).

The ^{1}H NMR spectrum of **3** is composed of two sets of pyrazolyl resonances of 2:1 intensity ratio, while one set of COD resonances is observed, indicating that fast pyrazolyl exchange takes place at room temperature in dichloromethane-d_2 (Figure 6, trace A). This situation remains unchanged until 257 K, below which two resonances from olefinic COD protons appear, whereas the 2:1 pattern of 4-H(pz) is still present. This evidences clearly the quenching of the (3-Ph,5-Mepz) ↔ (3-Me,5-Phpz) chemical exchange process leading to the in-plane asymmetry of COD. The (3-Ph,5-Mepz)$_{coord}$ ↔ (3-Ph,5-Mepz)$_{uncoord}$ exchange remains fast on the time scale of the method until 210 K, when simultaneously three resonances from 4-H(pz) and four resonances from olefinic COD protons appear (trace D). Thus, two separate chemical exchange processes corresponding to (3-Ph,5-Mepz) ↔ (3-Me,5-Phpz) and (3-Ph,5-Mepz)$_{coord}$ ↔ (3-Ph,5-Mepz)$_{uncoord}$ with the values of $\Delta G^{\ddagger}_{BC1} = 48.1$ kJ/mol and $\Delta G^{\ddagger}_{BC2} = 46.4$ kJ/mol are observed, respectively. This conclusion corroborates with 2D NMR COSY and NOESY experiments performed at 190 K, which showed the presence of both scalar and EXSY cross-peaks between a ↔ b and c ↔ d. Further insight into dynamic behavior of **3** is based on the observed three minor peaks in the region of 4-H(pz) resonances (trace E). Two sets of three 4-H(pz) resonances, as well as well-resolved resonances from *o*-H (3-Ph,5-Mepz), appear at the 88:12 intensity ratio at 190 K, and they correspond to two DR isomers resulted from dangling 3-Ph,5-Mepz. Their energies are different, consistent with the asymmetry imposed by the rest of molecule, which was absent in the case of **2**.

Finally, the in-plane asymmetry for the dominating DR isomer in **3** consistent with different *cis*- and *trans*-electronic and steric effects of two different coordinated pyrazoles induced a 0.65 ppm chemical shift difference (measured as $\Delta\delta_{BC1} = (\delta_a + \delta_b)/2 - (\delta_c + \delta_d)/2$), whereas the up-and-down asymmetry resulted in the average 0.26 ppm chemical shift nonequivalence of olefinic COD

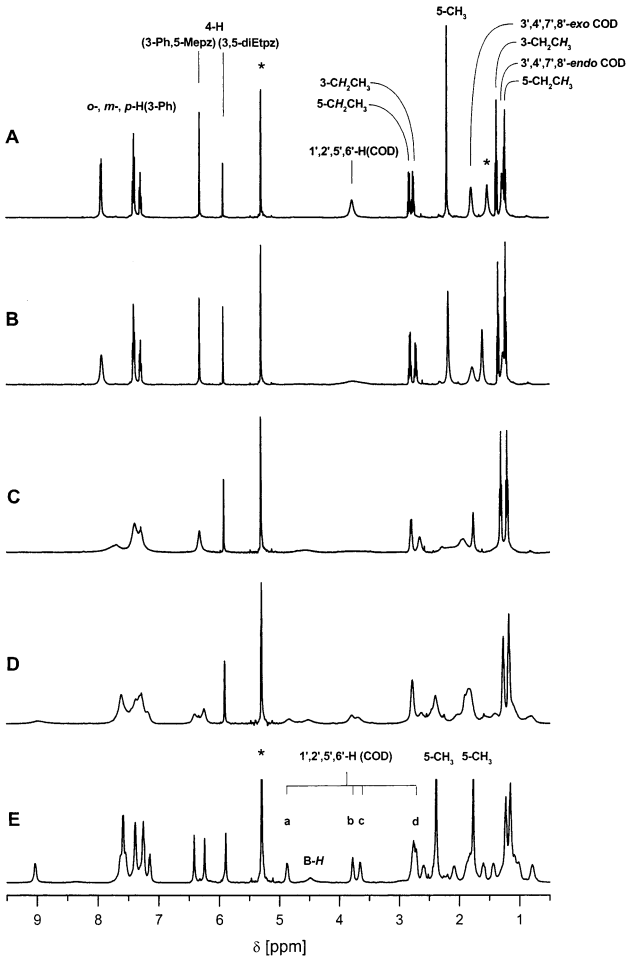

Figure 7. ^{1}H NMR spectra of **4** dichloromethane-d_2 at 300 K (A); 270 K (B); 230 K (C); 210 K (D); and 190 K (E). The residual peaks from the solvent and trace HDO are labeled with asterisks.

protons ($\Delta\delta_{ab} = 0.31$; $\Delta\delta_{cd} = 0.20$ ppm, mean $\Delta\delta_{BC2} = 0.25$ ppm), which was considerably smaller than in the case of **2**.

The ^{1}H NMR spectrum of **4** recorded at 300 K is composed of two 4-H resonances at 6.29 and 5.88 ppm of 2:1 intensity ratio and one set of COD resonances attributed to B or B ↔ C fast interconverting species (Figure 7, trace A). The assignment of resonances has been done on the basis of heteronuclear ^{1}H−^{13}C HMQC and HMBC experiments. Three resonances of the COD ligand, each of the intensity corresponding to four protons, are broad, which is rather typical for this kind of complexes. Variable-temperature experiments in dichloromethane-d_2 indicated that primarily the (3-Ph,5-Mepz) ↔ (3,5-diEtpz) exchange became slow on the time scale of the method at 255 K, resulting in the appearance of two olefinic proton resonances below that temperature with a preserved 2:1 pattern of 4-H(pz) resonances (traces B and C). The slow $(3\text{-Ph,5-Mepz})_{coord}$ ↔ $(3\text{-Ph,5-Mepz})_{uncoord}$ exchange at temperatures below 223 K accounts for the appearance of three 4-H(pz) and four olefinic proton resonances (labeled a−d in trace E). The scalar couplings within the a ↔ b and c ↔ d pairs of olefinic COD protons as cross-peaks in the COSY spectrum and the same pattern of EXSY cross-peaks in the NOESY spectrum are analogous to those for **3**. The values of activation energy corresponding to (3-Ph,5-Mepz) ↔ (3,5-diEtpz) and $(3\text{-Ph,5-Mepz})_{coord}$ ↔ $(3\text{-Ph,5-Mepz})_{uncoord}$ are equal to $\Delta G^{\ddagger}_{BC1} = 46.9$ kJ/mol and $\Delta G^{\ddagger}_{BC2} = 41.1$ kJ/mol, respectively.

A detailed analysis of the spectra indicate that average chemical shifts of the 4-H of uncoordinated and coordinated 3-Ph,5-Mepz and that of 4-H of 3,5-diEtpz remain unchanged upon slowing down the chemical exchange. On the other hand, the difference of the chemical shift of peripheral protons of 3-Ph,5-Mepz between the coordinated and uncoordinated moiety is rather large; the chemical shift difference of *o*-H(3-Ph) is as large as 1.44 ppm, whereas that for 5-CH_3 reaches 0.59 ppm. The chemical shift differences between COD protons are quite large; the 1.14 ppm gap between pairs of resonances corresponding to 1′,2′-H and 5′,6′-H ($\delta_{AB} - \delta_{CD}$, trace E) attributed to different *cis*−*trans* surroundings (no scalar cross-peaks were observed between 1′(2′) and 6′(5′) protons in the COSY spectrum) and the 1.10 ppm chemical shift difference between protons a and b (0.93 ppm for c and d) related to up-and-down asymmetry of the square planar complex were observed. These observations suggest that the chemical shift anisotropy in **4** originates from steric effects rather than from different electronic properties of coordinated pyrazolyl residues.

The values of $\Delta G^{\ddagger}_{BC1}$ in Tp′Rh(COD) complexes are considerably lower in comparison with those observed for $Tp^{Ph,Me}Rh(CO)(PPh_3)$[8] (76.5 kJ/mol), $Tp^{Me,Me}Rh(CO)(PMe_3)$[22] (63 kJ/mol), and $Tp(C_2H_4)(PPh_3)$[23] (60 kJ/mol). The $(pz)_{coord}$ ↔ $(pz)_{uncoord}$ exchange, corresponding to the mentioned B ↔ C interconversion, proceeds via an associative mechanism, with a pentacoordinate intermediate, presumably with the rhodium center at *tbp* geometry.[24] Therefore, the larger steric hindrance of the intermediate, the higher $\Delta G^{\ddagger}_{BC1}$ can be expected. The steric hindrance results both from Tp′ (Tp″) and from ancillary L_1L_2 ligands. In the case of $L_1L_2 = (CO)_2$ the $\Delta G^{\ddagger}_{BC}$ is too small to be detected by ^{1}H NMR spectroscopy, while in the case when $L_2 = PR_3$ the values of $\Delta G^{\ddagger}_{BC}$ are above 60 kJ/mol. The steric hindrance imposed by the symmetric COD ancillary ligand is intermediate, and consequently the $\Delta G^{\ddagger}_{BC1}$ values are at the level of 43−47 kJ/mol (for **2**−**4**). Due to C_1 symmetry of the stable species for **3** and **4** at low temperatures, the $\Delta G^{\ddagger}_{BC2}$ values could be estimated. The $\Delta G^{\ddagger}_{BC1} - \Delta G^{\ddagger}_{BC2}$ corresponds to a difference in steric hindrance between 3-Ph,5-Mepz and 3-Me,5-Phpz in **3** and 3-Ph,5-Mepz and 3,5-diEtpz in **4**. As one could expect, the difference for **4** is larger (5.8 kJ/mol) in comparison with that for **3** (2.3 kJ/mol). However, the values of $\Delta G^{\ddagger}_{BC1}$ and $\Delta G^{\ddagger}_{BC2}$ depend on the values of free energy of interconverting B forms, which bear different coordinating and dangling pyrazolyls.

It has been shown that the strength of Rh−N(pz) bonds can be largely differentiated, when two different *trans* ligands are coordinated, as it was the case in the molecule of $Tp^{Ph,Me}Rh(CO)(PPh_3)$, in which two stepwise $(3\text{-Ph,5-Mepz})_{coord}$ ↔ $(3\text{-Ph,5-Mepz})_{uncoord}$ equilibria were observed with an energy gap of 21 kJ/mol.[8] In the case of **2**−**4** the symmetric COD ancillary ligand does not

(22) Chauby, V.; Serra Le Berre, C.; Kalck, P.; Daran, J.-C.; Commenges, G. *Inorg. Chem.* **1996**, *35*, 6354.
(23) Oldham, W. J.; Heinekey, D. M. *Organometallics* **1997**, *16*, 467.
(24) Webster, C. E.; Hall, M. B. *Inorg. Chim. Acta* **2002**, *330*, 268.

introduce an additional variable; therefore the results on $\Delta G^{\ddagger}_{BC1} - \Delta G^{\ddagger}_{BC1}$ seem to be reliable.

Catalytic Tests. Catalytic activity in stereoregular polymerization of phenylacetylene (PA) to *cis*-transoidal poly(phenylacetylene) has been reported for the series of Tp′Rh(COD) complexes.[20] Following the same procedure we have found that **2**−**4** were also highly active as catalysts. Moreover, the catalysts were quite stable under the applied reaction conditions (193 K, 24 h, 140-fold excess of PA) and could be repeatedly used. The ^{1}H NMR monitoring of the catalytic reaction (12-fold excess of PA was used) by the disappearance of resonances from PA showed the absence of any other rhodium complex in the mixture other than the starting one. In addition, the release of the COD ligand was not noticed. The complex $Tp^{Ph,Me}Rh(CO)_2$ (entry 3), which was found to be catalytically inactive, may be converted in situ by addition of an equimolar amount of COD in the presence of PA (entries 4, 5). The immediate formation of **2** accompanied by polymerization of PA took place as followed by ^{1}H NMR. A similar catalytic experiment was performed with the use of a larger amount of COD without losing catalytic activity of **2**. The most efficient catalyst was **4**, for which the highest M_w values were obtained in test reaction conditions (entry 9). Currently we are studying the catalytic activity of Tp′Rh(L_1L_2) complexes in copolymerization of acetylenes. Other catalytic tests with **1** and [HB(3-Ph,5-Mepz)$_2$(3,5-diMepz)]Rh(CO)(PPh_3), formed in situ by addition of 1−4 equiv of PPh_3, indicated that complexes were inactive in hydrogenation and hydroformylation, in contrast to $[TpRu(PPh_3)_n(CH_3CN)_{3-n}]^+$ (where n = 2 or 1), which were evidenced to catalyze the hydrogenation of styrene and in situ-generated TpRh(COD), the species probably responsible for hydrogenative degradation of quinoline.[25,26]

Experimental Section

General Procedures. Syntheses of Tp′Rh(COD) and Tp′Rh(CO)$_2$ complexes were performed under nitrogen atmosphere using standard Schlenck and vacuum-line technique. The anionic ligands were synthesized as sodium salts: Na[HB(3-Ph,5-Mepz)$_2$(3,5-diMepz)],[27] Na[HB(3-Ph,5-Mepz)$_3$],[4] Na[HB(3-Ph,5-Mepz)$_2$(3-Me,5-Phpz)],[4] and Na[HB(3-Ph,5-Mepz)$_2$(3,5-diEtpz)],[28] by previously described procedures. [RhCl(COD)]$_2$ was synthesized according to published methods.[29] The $Tp^{Ph,Me}$Rh(CO)$_2$ was obtained as before.[8] NMR experiments were carried out on Bruker AMX 300 MHz and Bruker Avance 500 MHz instruments using standard parameters and pulse sequences for ^{1}H COSY and NOESY experiments and heteronuclear ^{1}H−^{13}C HMQC and HMBC experiments. The assignments of carbon resonances in ^{13}C NMR spectra for Tp″Rh(COD) complexes are in accordance with the numbering shown in Scheme 2. The FT IR spectra were recorded on a Perkin-Elmer 1725X instrument.

Syntheses of Complexes. 1. Na[HB(3-Ph,5-Mepz)$_2$(3,5-diMepz)] (200 mg, 0.45 mmol) dissolved in 15 mL of toluene was added slowly to a solution of Rh(acac)(CO)$_2$ (155.4 mg, 0.60 mmol) in toluene (15 mL). The mixture was stirred for 20 h at room temperature. The precipitate of Na(acac) was filtered off, and the filtrate was reconcentrated to a volume of 5 mL and left at 4 °C for 12 h. The resulting yellow precipitate was collected by filtration, washed with ethanol and diethyl ether, and vacuum-dried (250 mg, 0.43 mmol, 95% yield). Crystals suitable for crystallographic measurement were grown from concentrated toluene solution at 4 °C.

Anal. Calcd for $C_{27}H_{27}N_6O_2BRh$: C, 55.79; H, 4.68; N, 14.46. Found: C, 56.10; H, 4.59; N, 14.68. IR (KBr): 2552 cm^{-1} (ν_{B-H}); 2070 (s), 2016 (s) cm^{-1} (ν_{C-O}). ^{1}H NMR (toluene-d_8; δ): 7.85 (d, J = 7.1 Hz, 4H, *o*-H(3-Ph,5-Mepz)); 7.43−736 (m, 6H, *m*- and *p*-H(3-Ph,5-Mepz)); 6.33 (s, 2H, 4-H(3-Ph,5-Mepz)); 6.02 (s, 1H, 4-H(3,5-diMepz)); 4.82 (m, J_{BH} = 150 Hz, B-*H*); 2.48, 2.47 (s, s, 3H, 3H, 3- and 5-CH_3(3,5-diMepz)); 2.44 (s, 6H, 5-CH_3(3-Ph,5-Mepz)).

2. The complex was synthesized at 83% yield (at the 0.21 mmol of $NaTp^{Ph,Me}$ scale) according to a published procedure, except benzene instead of dichloromethane[10] or acetonitrile[17] was used as the solvent for reaction between [RhCl(COD)]$_2$ and $NaTp^{Ph,Me}$. Crystals of **2** were grown from a benzene−hexane mixture. Satisfactory elemental analysis and IR and ^{1}H NMR spectra confirmed the purity of **2**.[10]

Anal. Calcd for $C_{38}H_{40}N_6BRh$: C, 65.72; H, 5.81; N, 12.10. Found: C, 66.17; H, 6.02; N, 12.06.

3. 3 was synthesized by stirring Na[HB(3-Ph,5-Mepz)$_2$(3-Me,5-Phpz)] (0.105 g, 0.207 mmol) with [RhCl(COD)] (0.045 g, 0.095 mmol) in 4 mL of benzene for 3 h at room temperature. The precipitate of NaCl was filtered off, the filtrate was twice concentrated under a stream of nitrogen, and the solution was layered with ca. 2.5 mL of hexane. Yellow crystals of analytically pure **3** were collected (0.111 g, 0.160 mmol, 84% yield). Crystals of **3**·CH_2Cl_2 suitable for X-ray crystallographic measurement were obtained by recrystallization of **3** from a dichloromethane−hexane solvent mixture.

Anal. Calcd for $C_{39}H_{42}N_6Cl_2BRh$: C, 60.10; H, 5.43; N, 10.78. Found: C, 60.16; H, 5.46; N, 10.38. IR (KBr): 2481 cm^{-1} (ν_{B-H}). ^{1}H NMR (300 K, dichloromethane-d_2; δ): 7.92 (d, J = 7.1 Hz, 4H, *o*-H(3-Ph,5-Mepz)); 7.58 (d, J = 7.1 Hz, 2H, *o*-H(3-Me,5-Phpz)); 7.44−7.28 (m, 6H, *m*-, *p*-H(3-Ph,5-Mepz and 3-Me,5-Phpz)); 6.29 (s, 2H, 4-H(3-Ph,5-Mepz)); 6.14 (s, 1H, 4-H(3-Me,5-Phpz)); 3.80 (br s, 4H, 1′, 2′, 5′, 6′-H (COD)); 2.59 (s, 3H, 3-CH_3(3-Me,5-Phpz)); 2.03 (s, 6H, 5-CH_3(3-Ph,5-Mepz)); 1.85

Scheme 2

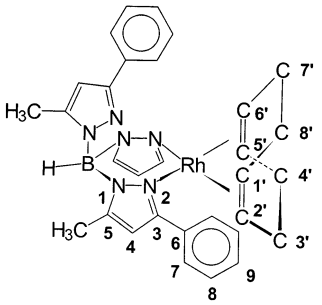

Table 2. Catalytic Data

entry	catalyst	yield (%)[a]	M_w[b]	M_w/M_n[c]
1	**2**	96	47 000	2.38
2	**2**, reused	86	39 300	2.77
3	$Tp^{Ph,Me}Rh(CO)_2$ (**2′**)	0		
4	**2′** + COD (2.5 equiv)	72	71 300	1.97
5	**2′** + COD (5.0 equiv)	100	25 400	1.84
6	**3**	98	19 000	2.03
7	**3**, reused	83	15 000	1.97
8	**3**, reused second time	100	40 000	2.05
9	**4**	100	84 600	2.48

[a] % of *cis*-poly(phenylacetylene) found by ^{1}H NMR was 95−100. [b] M_w, molecular weight of polymer. [c] M_w/M_n, polydispersity.

(25) Chan, W.-C.; Lau, C.-P.; Che, Y.-Z.; Fang, Y.-Q.; Ng, S.-M.; Jia, G. *Organometallics* **1997**, *16*, 34.
(26) Alvarado, Y.; Busolo, M.; Lopez-Linares, F. *J. Mol. Catal. A* **1999**, *142*, 163.
(27) Łukasiewicz, M.; Ciunik, Z.; Ruman, T.; Skóra, M.; Wołowiec, S. *Polyhedron* **2001**, *20*, 237.
(28) Ruman, T.; Ciunik, Z.; Wołowiec, S. *Polyhedron* **2002**, *21*, in press (Part IX).
(29) Giordano, G.; Crabtree, R. H. *Inorg. Synth.* **1990**, *28*, 88.

Table 3. Crystal Data and Structure Refinement

	1	**2**	**3**·CH_2Cl_2	**4**
empirical formula	$C_{27}H_{26}BN_6O_2Rh$	$C_{38}H_{40}BN_6Rh$	$C_{39}H_{42}BN_6Cl_2Rh$	$C_{35}H_{42}BN_6Rh$
fw	581.27	694.48	779.41	660.47
T/K	100(2)	100(2)	100(2)	100(2)
λ/Å	0.71073	0.71073	0.71073	0.71073
cryst syst	monoclinic	monoclinic	triclinic	triclinic
space group	$P2_1/c$	$P2_1/c$	$P\bar{1}$	$P\bar{1}$
a/Å	12.6077(7)	11.5038(8)	12.872(2)	9.9159(7)
b/Å	19.6436(10)	15.1991(8)	12.906(2)	12.7807(8)
c/Å	11.2120(7)	19.1803(10)	12.9910(19)	13.8793(12)
α/deg			107.272(14)	65.288(7)
β/deg	105.554(5)	100.626(5)	96.892(13)	76.741(7)
γ/deg			113.646(13)	79.880(6)
V/Å^3	2675.1(3)	3296.1(3)	1816.0(5)	1548.9(2)
Z	4	4	2	2
D_c/Mg·m^{-3}	1.443	1.399	1.425	1.416
μ/mm^{-1}	0.674	0.555	0.655	0.587
F(000)	1188	1440	804	688
cryst size/mm	0.19 × 0.16 × 0.13	0.18 × 0.18 × 0.10	0.18 × 0.15 × 0.13	0.17 × 0.14 × 0.12
θ range for data collection/deg	3.51−28.51	3.34−28.50	3.31−28.45	3.58−28.30
ranges of h,k,l	−16→16,−25→20, −14→14	−10→15,−20→20, −24→25	−17→16,−12→17, −16→17	−13→13,−15→15, −18→14
no. of reflns collected	18 275	22 423	12 679	9162
no. of ind reflns	6196 (0.0320)	7734 (0.0269)	7984 (0.0336)	6163 (0.0192)
no. of data/params	6196/338	7734/575	7984/610	6163/556
GOF(F^2)	1.099	1.091	0.953	1.040
final R_1/wR_2 indices ($I>2\sigma_I$)	0.0295/0.0694	0.0293/0.0674	0.0414/0.0603	0.0242/0.0555
largest diff peak/hole/e·Å^{-3}	1.011/−0.753	0.984/−0.591	0.761/−0.577	0.957/−0.472

(br m, 4H, 3′, 4′, 7′, 8′-H_{exo} (COD)); 1.33 (m, 4H, 3′, 4′, 7′, 8′-H_{endo} (COD)). ^{13}C NMR (300 K, dichloromethane-d_2; δ): 153.2 C-3(3-Ph,5-Mepz); 152.6 C-3(3-Me,5-Phpz); 150.9 C-5(3-Me,5-Phpz); 146.6 C-5(3-Ph,5-Mepz); 135.7 C-6(3-Ph,5-Mepz); 133.7 C-6(3-Me,5-Phpz); 130.3 C-7(3-Me,5-Phpz); 129.0 C-7(3-Ph,5-Mepz); 128.6 C-9(3-Me,5-Phpz); 128.5 C-8(3-Me,5-Phpz); 128.2 C-9(3-Ph,5-Mepz); 127.9 C-8(3-Ph,5-Mepz); 108.1 C-4(3-Me,5-Phpz); 106.3 C-4(3-Ph,5-Mepz); 81.7 C-1′,2′,5′,6′ (COD); 30.1 C-3′,4′,7′,8′ (COD); 15.9 3-CH_3(3-Me,5-Phpz); 13.4 5-CH_3(3-Ph,5-Mepz).

4. The complex was synthesized as **3** at the scale of 0.115 g of Na[HB(3-Ph,5-Mepz)$_2$(3,5-diEtpz) (0.24 mmol) and 0.049 g of [RhCl(COD)]$_2$ (0.10 mmol). Analytically pure **4** was obtained by crystallization from benzene−hexane (yield 0.120 g, 0.182 mmol, 91% yield).

Anal. Calcd for $C_{35}H_{42}N_6BRh$: C, 63.65; H, 6.41; N, 12.72. Found: C, 63.47; H, 6.68; N, 12.59. IR (KBr): 2484 cm^{-1} (ν_{B-H}). ^{1}H NMR (300 K, dichloromethane-d_2; δ): 7.94 (d, J = 7.1 Hz, 4H, *o*-H(3-Ph,5-Mepz)); 7.42−7.28 (m, 6H, *m*-, *p*-H(3-Ph,5-Mepz)); 6.32 (s, 2H, 4-H(3-Ph,5-Mepz)); 5.93 (s, 1H, 4-H(3,5-diEtpz)); 4.60 (m, J_{BH} = 140 Hz, 1H, B-*H*) 3.78 (br s, 4H, 1′, 2′, 5′, 6′-H (COD)); 2.80 (q, J = 7.6 Hz, 2H, 3-CH_2CH$_3$(3,5-diEtpz); 2.74 (q, J = 7.6 Hz, 2H, 5-CH_2CH$_3$(3,5-diEtpz); 2.20 (s, 6H, 5-CH_3(3-Ph,5-Mepz)); 1.79 (br s, 4H, 3′, 4′, 7′, 8′-H_{exo} (COD)); 1.38 (t, 3H, 5-CH$_2$CH_3(3,5-diEtpz); 1.27 (m, 4H, 3′, 4′, 7′, 8′-H_{endo} (COD)); 1.23 (t, 3H, 3-CH$_2$CH_3(3,5-diEtpz). ^{13}C NMR (300 K, dichloromethane-d_2; δ): 155.7 C-5(3,5-diEtpz); 152.7 C-3(3,5-diEtpz); 152.1 C-5(3-Ph,5-Mepz)); 145.6 C-3(3-Ph,5-Mepz)); 135.0 C-6(3-Ph); 128.1 C-7(3-Ph); 127.1 C-8(3-Ph); 126.9 C-9(3-Ph); 103.3 C-4(3,5-diEtpz); 105.1 C-4(3-Ph,5-Mepz); 80.5 C-1′,2′,5′,6′ (COD); 29.4 C-3′,4′,7′,8′ (COD); 22.1 5-*C*H$_2$CH$_3$(3,5-diEtpz); 21.1 3-*C*H$_2$CH$_3$(3,5-diEtpz); 14.5. 5-CH$_2$*C*H$_3$(3,5-diEtpz); 13.2 3-CH$_2$*C*H$_3$(3,5-diEtpz); 12.9 5-*C*H$_3$-(3-Ph,5-Mepz).

Catalytic Procedures. Complexes **1**−**4** were tested for catalytic activity in the polymerization of phenylacetylene (PA). In a typical experiment 0.013 mmol of catalyst was dissolved in 0.5 mL of CH_2Cl_2, and 0.2 mL of PA (1.82 mmol) was added. The mixture was stirred under nitrogen at 293 K for 24 h, then the polymer was precipitated by addition of methanol (2 mL), separated by microfiltration, washed with methanol, weighed in order to determine the yield, and analyzed for number- and weight-average molecular weights (M_n and M_w) and polydispersity (M_n/M_w) with the use of a Hewlett-Packard GPC system ($CHCl_3$ solutions), a refractive index detector, and a Plgel 10 m MIXED-B column The reuse of catalysts tests was performed by stripping out the volatiles from the filtrate and addition of CH_2Cl_2 and PA as in the primary tests. Finally, the polymer samples were analyzed by ^{1}H NMR spectroscopy in chloroform-*d* to establish the percentage of *cis*-poly(phenylacetylene) in accordance with published procedures.[30]

In a separate experiment 3 mg of **2** and a 12-fold excess of PA in dichloromethane-d_2 were used, and the progress of the reaction was monitored by ^{1}H NMR spectroscopy. The progress of polymerization was followed by the disappearance of the substrate peak at 3.05 ppm and growing of the resonances from poly(phenylacetylene) at 5.9, 6.7, and 6.9 ppm. Throughout 24 h of monitoring the PA resonance disappeared, while the resonances from **2** remained unchanged. Formation of free COD was not observed (absence of resonances at 2.4 and 5.6 ppm).

In another experiment **2** was generated in situ by addition of an equimolar amount of COD into the solution of Tp^{Ph,Me}-Rh(CO)$_2$. The formation of **2** was observed immediately by peaks of coordinated COD at 3.30, 1.60, and 1.09 ppm, which remained unchanged over a period of 24 h, while the PA (added at 12-fold excess together with COD) was totally consumed in the catalytic reaction. The results of catalytic tests on the polymerization of PA are summarized in Table 2.

Compound **1** and [HB(3-Ph,5-Mepz)$_2$(3,5-diMepz)]Rh(CO)-(PPh_3) generated in situ by addition of 1 equiv of PPh_3 were tested for catalytic activity in the hydrogenation and hydroformylation of hex-1-ene in toluene (3−7 h, 353 K) and acetone (72 h, 353 K). Standard conditions for catalytic runs were 0.01−0.02 g of catalyst, 1.5 mL of hexane, 1.5 mL of solvent, and 10 atm pressure of H_2/CO = 1.

Experimental Procedure for X-ray Crystallography. Suitable crystals of **1**, **2**, **3**, and **4** were glued on top of a glass fiber and transferred into the cold nitrogen stream on a Kuma KM4CCD κ-axis diffractometer (graphite-monochromated Mo Kα radiation, λ = 0.71073 Å). Crystals were positioned at 65 mm from the CCD camera. A total of 612 frames were

(30) Furlani, A.; Licoccia, S.; C.; Russo, M. V. *J. Polym. Sci., Part A: Polym. Chem.* **1986**, *24*, 991.

measured at 0.75° intervals with a counting time of 10−15 s. Accurate cell parameters were determined and refined by least-squares fit of 2700−5100 of the strongest reflections. Data were corrected for Lorentz and polarization effects. No absorption corrections were applied. Data reduction and analysis were carried out with the Oxford Diffraction (Poland) (formerly Kuma Diffraction Wrocław, Poland) programs. The structures were solved by the heavy method (program SHELXS97[31]) and refined by the full-matrix least-squares method on all F^2 data using the SHELXL97 programs.[32] Non-hydrogen atoms were refined with anisotropic displacement parameters; hydrogen atoms were included from geometry of molecules and/or $\Delta\rho$ maps. Their parameters were not refined in **1**, and in **2**, **3**, and **4** they were refined isotropically. Neutral atom scattering factors were taken from Cromer and Waber.[33] Final refinement details are collected in Table 1, and the numbering schemes employed are shown in Figures 1, 2, 3, and 4, which were drawn with ORTEP as 30% probability ellipsoids.

Additional Materials. Crystallographic data for the structures reported in this paper have been deposited with the Cambridge Crystallographic Data Centre, CCDC no. 192815 for compound **1**, CCDC no. 192816 for **2** , CCDC no. 192817 for **3**·CH_2Cl_2, and CCDC no. 192818 for **4**. Copies of this information may be obtained free of charge from the Director, CCDC, 12 Union Rd., Cambridge 1EZ, UK (fax: +44-1223-336033; e-mail: deposit@ccdc.cam.ac.uk or http://www.ccdc.cam.ac.uk).

Acknowledgment. This work was supported by State Committee for Scientific Research KBN (Poland) with Grants 3T09A 05219 to T.R., Z.C., A.T., and S.W., and PBZ KBN 15/T09/99/01D to A.T. and J.J.Z.

Supporting Information Available: Crystallographic data. This material is available free of charge via the Internet at http://pubs.acs.org.

OM020873X

(31) Sheldrick, G. M. *SHELXS97*: Program for Solution of Crystal Structures; University of Göttingen, 1997.

(32) Sheldrick, G. M. *SHELXL97*: Program for Crystal Structure Refinement; University of Göttingen, 1997.

(33) Cromer, D. T.; Waber, J. T. *International Tables for X-ray Crystallography*; Kynoch Press: Birmingham, U.K., 1974; Vol. 4.